Progress In Electromagnetics Research M, Vol. 101, 101–115, 2021

Full Wave Analysis of Multilayered Cylindrical Resonator Containing Uniaxial Anisotropic Media

Krzysztof Derzakowski*

Abstract—The method of evaluating the resonant frequencies of a multilayered cylindrical resonator containing uniaxial anisotropic materials is presented. The detailed solution of Maxwell's equations for such a structure by means of the radial mode matching method is given. The results of calculations using developed and launched computer program are given, and they are compared with those obtained by other methods and with measurements. These results are in close agreement, which proves the correctness of the method. The developed solution and the software program can be used to measure the permittivity tensor of materials.

1. INTRODUCTION

The development of materials technology makes that newly created materials have previously unattainable electrical properties. They are very quickly adapted to the fabrication and construction of systems in the field of electronics. Dielectric materials produced and used in electronics have a wide range of relative permittivity — from a few to a few thousands and the loss tangent — from a few to 10^{-7}. These parameters may vary depending on the frequency as well as a function of the direction (anisotropic materials) and the applied external electric field (ferroelectrics). The use of such materials in electronics enforces the need for accurate knowledge of their electrical parameters. It is therefore necessary to develop newer and better methods to measure these materials.

At microwave frequencies, for dielectric with a relative permittivity greater than 10, resonant methods are most often used, in particular dielectric resonator method [1]. The advantage of this method has very good accuracy to determine material parameters, and the measurements are easy. The resonant frequency and Q-factor of the structure, which includes sample test material are measured at once [2]. The material parameters are determined from the equations describing the resonance conditions of the test structure. There are many ways to derive these equations; however, the most accurate ones appear to be mode matching methods, either radial or axial.

In the literature there are numerous studies enabling the calculation of the resonant frequency of the structure used in the measurement, but most commonly they involve a simple structure composed of a small number of layers of material, for example: post dielectric resonator [3], microstrip line structure [4], and the like. The most advanced solution relates to a multilayer dielectric resonator which can contain up to 10 regions and 10 layers in each of them, but dielectrics included in the system are described by scalar relative permittivity [5, 6].

It is possible to use any electromagnetic simulator, e.g., CST [7], QuickWave [8], HFFS [9], to calculate the resonant frequency of a complex structure. However, each of these simulators uses approximations of partial differential equations, so the accuracy of the calculations is limited. In 3D simulators, the structure is meshed, and accuracy of the computations depends on the mesh size. Thus,

Received 8 December 2020, Accepted 2 February 2021, Scheduled 23 February 2021
* Corresponding author: Krzysztof Derzakowski (k.derzakowski@ire.pw.edu.pl).
The author is with the Institute of Radioelectronics and Multimedia Technology, Warsaw University of Technology, ul. Nowowiejska 15/19, Warsaw 00-665, Poland.

the accuracy depends on the quantization of space. It can also depend on the quantization of time (in FDTD), dispersion, round-off errors, etc. The computation time in some simulators may be much longer than in the presented solution. The price of commercial electromagnetic simulators is also an important factor, but it must be added that the 3D electromagnetic simulators can be used to any type of structures, which is their main advantage.

In this paper, a solution employing the radial mode matching method for the multilayered resonator containing materials with tensor permittivity, with assumed uniaxial anisotropy, is presented. Although studies on the structure containing uniaxial anisotropic materials are presented in the literature, they are related to simple structures [10–15]. In this work, a solution of the Maxwell equations for the multilayered resonator, which may contain up to 20 regions and 20 layers of each of them, which is more than exhaustive demand is presented.

2. THE SOLUTION OF BOUNDARY VALUE PROBLEM FOR THE RESONATOR WITH ANISOTROPIC MEDIA

The simplified general structure of the multilayered dielectric resonator is shown in Fig. 1.

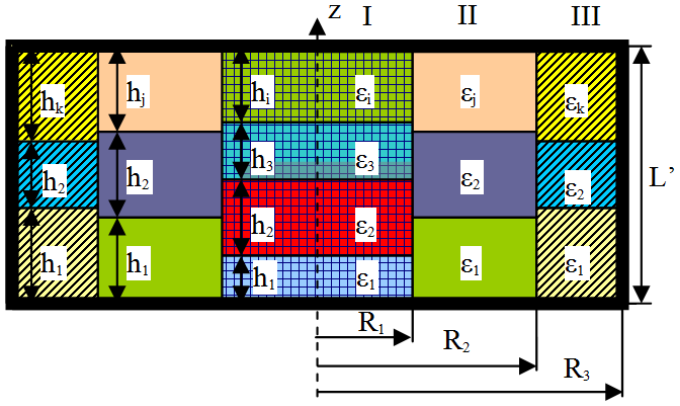

Figure 1. Multilayered dielectric resonator.

It consists of three regions I, II, and III with axial symmetry. The number of these regions can be equal to a maximum of 20 in the developed program. The first region thus has a cylindrical shape, and the next ones are rings. In each region there is a number of layers of material having different relative complex tensor permittivities. The structure is enclosed by a metal cylinder whose radius R_3 may be infinite. The structure does not affect constant or slowly varies external magnetic field.

The solution of structure shown in Fig. 1 makes possible to determine the resonant frequency f_o of all modes and additionally corresponding components of the electromagnetic field.

The stated problem boils down to solving Maxwell's equations for such a structure. Due to the rotational symmetry of the analyzed structure, the Maxwell equations will be solved in a cylindrical coordinate system.

Maxwell's equations in each layer of each region can be written as (given the absence of charges and currents sources):

$$\begin{cases} \nabla \times \vec{E} = -j\omega\vec{B} & (1) \\ \nabla \times \vec{H} = j\omega\vec{D} & (2) \\ \nabla \cdot \vec{D} = 0 & (3) \\ \nabla \cdot \vec{B} = 0 & (4) \end{cases}$$

Taking into account the linearity and anisotropy of the media belonging to the resonator and the

lack of magnetic properties, the following is obtained:

$$\begin{cases} \nabla \times \vec{E} = -j\omega\mu_o\vec{H} & (5) \\ \nabla \times \vec{H} = j\omega\bar{\bar{\varepsilon}}\vec{E} & (6) \\ \nabla \cdot (\bar{\bar{\varepsilon}}\vec{E}) = 0 & (7) \\ \nabla \cdot \vec{H} = 0 & (8) \end{cases}$$

where: $\bar{\bar{\varepsilon}} = \begin{bmatrix} \varepsilon_t & 0 & 0 \\ 0 & \varepsilon_t & 0 \\ 0 & 0 & \varepsilon_z \end{bmatrix}$ is a complex permittivity tensor of uniaxial anisotropic medium.

Transforming $(5 \div 8)$ using vector calculus and field properties in the medium, finally we obtain two equations for the E_z and H_z components in the form:

$$\frac{1}{r}\frac{\partial}{\partial r}\left(r\frac{\partial E_z}{\partial r}\right) + \frac{1}{r^2}\frac{\partial^2 E_z}{\partial \varphi^2} + \frac{\varepsilon_z}{\varepsilon_t}\frac{\partial^2 E_z}{\partial z^2} + \omega^2\mu_0\varepsilon_0\varepsilon_z E_z = 0 \quad (9)$$

$$\frac{1}{r}\frac{\partial}{\partial r}\left(r\frac{\partial H_z}{\partial r}\right) + \frac{1}{r^2}\frac{\partial^2 H_z}{\partial \varphi^2} + \frac{\partial^2 H_z}{\partial z^2} + \omega^2\mu_0\varepsilon_0\varepsilon_t H_z = 0 \quad (10)$$

The remaining components are determined from Eqs. (5) and (6). After solving these equations in a cylindrical coordinate system and making transformations, we obtain:

$$\frac{\partial^2 E_\varphi}{\partial z^2} + \omega^2\varepsilon_o\varepsilon_t\mu_o E_\varphi = \frac{1}{r}\frac{\partial^2 E_z}{\partial z\partial\varphi} + j\omega\mu_o\frac{\partial H_z}{\partial r} \quad (11)$$

$$\frac{\partial^2 E_r}{\partial z^2} + \omega^2\varepsilon_o\varepsilon_t\mu_o E_r = \frac{\partial^2 E_z}{\partial z\partial r} - j\omega\mu_o\frac{1}{r}\frac{\partial H_z}{\partial\varphi} \quad (12)$$

$$\frac{\partial^2 H_\varphi}{\partial z^2} + \omega^2\varepsilon_o\varepsilon_t\mu_o H_\varphi = \frac{1}{r}\frac{\partial^2 H_z}{\partial z\partial\varphi} - j\omega\varepsilon_o\varepsilon_t\frac{\partial E_z}{\partial r} \quad (13)$$

$$\frac{\partial^2 H_r}{\partial z^2} + \omega^2\varepsilon_o\varepsilon_t\mu_o H_r = \frac{\partial^2 H_z}{\partial z\partial r} + j\omega\varepsilon_o\varepsilon_t\frac{1}{r}\frac{\partial E_z}{\partial\varphi} \quad (14)$$

Equations (9) and (10) are solved separately in each layer of each of the regions by using the method of separation of variables, and then the solutions are "stitched" on the borders of regions ($r = R_1$, $R = R_2$), ensuring continuity of tangential components. Assuming that in Equation (9) $E_z(r,\varphi,z) = R_e(r) * F_e(\varphi) * \Psi(z)$, we obtain a system of three equations depending only on single variable each:

$$\frac{d^2F_e(\varphi)}{d\varphi^2} + m^2F_e(\varphi) = 0 \quad (15)$$

$$r^2\frac{d^2R_e(r)}{dr^2} + r\frac{dR_e(r)}{dr} + (tr^2 - m^2)R_e(r) = 0 \quad (16)$$

$$\frac{d^2\Psi(z)}{dz^2} + \left(k_0^2\varepsilon_t - \frac{\varepsilon_t}{\varepsilon_z}t\right)\Psi(z) = 0 \quad (17)$$

where: $k_o^2 = \omega^2\varepsilon_o\mu_o$.

The solution of Equation (15) can be written as: $F_e(\varphi) = a_1\cos(m\varphi + \varphi_o)$, where a_1 and φ_0 are constants. Due to the required periodicity of the function $F_e(\varphi) = a_1\cos(m\varphi + \varphi_o)$ value m must be integer $m = 0, 1, 2, ...$

Equation (16) is for $t > 0$, the Bessel equation of the m-th order, and for $t < 0$, the modified Bessel equation of the m-th order. Its solutions for $t > 0$ are Bessel functions of the first kind of the m-th order — $J_m(\sqrt{t}r)$ and Neumann functions (Bessel functions of the second kind) of m-th order — $N_m(\sqrt{t}r)$. And for $t < 0$ solutions of Eq. (16) are modified Bessel functions of the first kind of the m-th order — $I_m(\sqrt{t}r)$ and the second kind of the m-th order — $K_m(\sqrt{t}r)$. It should be noticed that for the I-st region taking into account the Neumann function is not justified physically.

In each layer of the region, a permittivity is constant, and the solution of Eq. (17) is a set of functions $\Psi_n(z)$ that are a linear combination of trigonometric functions $\sin(v_{n_i}z)$ and $\cos(v_{n_i}z)$ type, wherein:

$$v_{n_i}^2 = k_o^2\varepsilon_t - \frac{\varepsilon_{t_i}}{\varepsilon_{z_i}}t_n \quad (i = 1, 2, ..., M,\ n = 0, 1, 2, ...)$$

If $\nu_{n_i}^2 < 0$, trigonometric functions should be replaced by the corresponding hyperbolic functions, i.e., $\sinh(v_{n_i}z)$ and $\cosh(v_{n_i}z)$. Since functions $\Psi_n(z)$ must be defined for the entire height of the region, we must ensure appropriate conditions of continuity on the electrical walls and separation planes of the various layers. These conditions are identical to those for the E_z component of the electromagnetic field, i.e.,

$\varepsilon_z^-\Psi^-(l_i) = \varepsilon_z^+\Psi^+(l_i)$ — step change on the border of separation of layers;
$\Psi'(0) = \Psi'(L') = 0$ — the disappearance of the derivative on the surface of the metal planes

where: $\Psi^-, \Psi'^-, \Psi^+, \Psi'^+$ — are values of the function Ψ and its derivative on the left and right hand side of the border between layers, $l_i = \sum_{p=1}^{i} h_i$ (i — number of a layer).

The fulfillment of these conditions is reflected in the function $\Psi_n(z)$ for the region. t_n values for which one can construct the desired function $\Psi_n(z)$ must have appropriate values. These are called eigenvalues of Eq. (17), and the corresponding functions are called eigenfunctions. All eigenvalues form an infinite sequence of values decreasing.

Completely analogously, one can solve Eq. (10), assuming an H_z component of the form:

$$H_z(r, \varphi, z) = R_n(r) * F_n(\varphi) * \Phi(z).$$

Finally a system of three equations of a single variable is obtained:

$$\frac{d^2F_n(\varphi)}{d\varphi^2} + m^2F_n(\varphi) = 0 \tag{18}$$

$$r^2\frac{d^2R_n(r)}{dr^2} + r\frac{dR_n(r)}{dr} + (\lambda r^2 - m^2)R_n(r) = 0 \tag{19}$$

$$\frac{d^2\Phi(z)}{dz^2} + (k_0^2\varepsilon_t - \lambda)\Phi(z) = 0 \tag{20}$$

Equations (18) and (19) are solved identically to Eqs. (15) and (16), but in Eq. (19) the argument will be equal to $\sqrt{\lambda}r$.

Differences between the solution of Eq. (20) and the solution of Eq. (17) due to different boundary conditions are fulfilled by the components H_z and E_z. Function $\Phi_n(z)$, fulfilling the same conditions as H_z must be:

- continuous on the boundary separating layers: $\Phi^-(l_i) = \Phi^+(l_i)$
- satisfy the requirement to disappear on the surfaces of metal plates: $\Phi(0) = \Phi(L')$

where: $\Phi^-, \Phi'^-, \Phi^+, \Phi'^+$ — are values of a function Φ and its derivative on the left and right hand sides of the boundary.

Thus components E_z and H_z can be represented as:

$$E_z(r, \varphi, z) = A\cos(m\varphi + \psi_o)\Psi_n(z)B_m(\sqrt{t_n}r) \tag{21}$$

$$H_z(r, \varphi, z) = B\sin(m\varphi + \varphi_o)\Phi_n(z)B_m(\sqrt{\lambda_n}r) \tag{22}$$

where: $B(x)$ — is the Bessel function.

Other field components are calculated from Eqs. (11)–(14). When these equations are solved, variables r and φ should be treated as parameters. Each of these equations (assuming that $E_z \neq 0$ and $H_z \neq 0$) can be written as an inhomogeneous equation of the second order in the following form:

$$\frac{\partial^2G(r, \varphi, z)}{\partial z^2} + k_0^2\varepsilon_t(z)G(r, \varphi, z) = P(r, \varphi, z) \tag{23}$$

The function $P(r,\varphi,z)$ is known, calculated using the formulas for components E_z and H_z and dependencies in Eqs. (15), (16), and (17) (right hand side) of the following form:

$$P(r,\varphi,z) = P_1(r,\varphi)\xi_{\Psi_n}(z) + P_2(r,\varphi)\xi_{\Phi_n}(z) \tag{24}$$

where — depending on the solved equation (11÷14) — $\xi_{\Psi_n}(z)$ means a function $\varepsilon_t(z)\Psi_n(z)$ or $\Psi'_n(z)$, and $\xi_{\Phi_n}(z)$ functions $\Phi_n(z)$ or $\Phi'_n(z)$. These functions are determined by Equations (15)–(17) substitution depending on the components $E_z(r,\varphi,z)$ and $H_z(r,\varphi,z)$. For example, for Equation (11), Equation (23) takes the form:

$$\frac{\partial^2 E_\varphi(r,\varphi,z)}{\partial z^2} + k_o^2\varepsilon_t(z)E_\varphi(r,\varphi,z) = \frac{1}{r}\frac{\partial^2 E_z(r,\varphi,z)}{\partial z\partial\varphi} + j\omega\mu_o\frac{\partial H_z(r,\varphi,z)}{\partial r} \tag{25}$$

Substituting $E_z(r,\varphi,z)$ and $H_z(r,\varphi,z)$, and performing simple transformations, we obtain:

$$\begin{aligned}\frac{\partial^2 E_\varphi(r,\varphi,z)}{\partial z^2} + k_0^2\varepsilon_t(z)E_\varphi(r,\varphi,z) \;=\; & -\frac{1}{r}Am\sin(m\varphi+\psi_0)\Psi'_n(z)B_m(\sqrt{t_n}r) \\ & +j\omega\mu_0 B\sqrt{\lambda_n}\sin(m\varphi+\varphi_0)\Phi_n(z)B'_m(\sqrt{\lambda_n}r)\end{aligned} \tag{26}$$

Hence:

$$\begin{aligned}P(r,\varphi,z) \;&=\; -\frac{1}{r}Am\sin(m\varphi+\psi_o)\Psi'_n(z)B_m(\sqrt{t_n}r) + j\omega\mu_o B\sqrt{\lambda_n}\sin(m\varphi+\varphi_o)\Phi_n(z)B'_m(\sqrt{\lambda_n}r) \\ P_1(r,\varphi) \;&=\; -\frac{1}{r}Am\sin(m\varphi+\psi_o)B_m(\sqrt{t_n}r), \\ P_2(r,\varphi) \;&=\; j\omega\mu_o B\sqrt{\lambda_n}\sin(m\varphi+\varphi_o)B'_m(\sqrt{\lambda_n}r)\end{aligned}$$

and $\xi_{\Psi_n}(z) = \Psi'_n(z)$, $\xi_{\Phi_n}(z) = \Phi_n(z)$.

The particular solution of the differential Equation (23) is the following function:

$$G(r,\varphi,z) = \frac{\varepsilon_z}{\varepsilon_t}\frac{1}{t_n}P_1(r,\varphi)\xi_{\Psi_n}(z) + \frac{1}{\lambda_n}P_2(r,\varphi)\xi_{\Phi_n}(z) \tag{27}$$

what can be proved by substituting this function to Eq. (23).

The electromagnetic field distribution in each region can be represented as an infinite linear combination of all radial waveguide modes E^α_{mn} and H^α_{mn} (where $\alpha = I, II, ..., XX$), so the components of the electromagnetic field can be written as:

$$E_z^{(\alpha)}(r,\varphi,z) = \sum_{i=0}^{\infty}\left[a_i^{(\alpha)}J_m\left(\sqrt{t_i^{(\alpha)}}r\right) + b_i^{(\alpha)}N_m\left(\sqrt{t_i^{(\alpha)}}r\right)\right]\Psi_i^{(\alpha)}(z)\cos\left(m\varphi+\psi_i^{(\alpha)}\right) \tag{28}$$

$$H_z^{(\alpha)}(r,\varphi,z) = \sum_{i=1}^{\infty}\left[c_i^{(\alpha)}J_m\left(\sqrt{\lambda_i^{(\alpha)}}r\right) + d_i^{(\alpha)}N_m\left(\sqrt{\lambda_i^{(\alpha)}}r\right)\right]\Phi_i^{(\alpha)}(z)\sin\left(m\varphi+\varphi_i^{(\alpha)}\right) \tag{29}$$

$$\begin{aligned}E_\varphi^{(\alpha)}(r,\varphi,z) = & \sum_{i=1}^{\infty}\frac{j\omega\mu_0}{\sqrt{\lambda_i^{(\alpha)}}}\left[c_i^{(\alpha)}J'_m\left(\sqrt{\lambda_i^{(\alpha)}}r\right) + d_i^{(\alpha)}N'_m\left(\sqrt{\lambda_i^{(\alpha)}}r\right)\right]\Phi_i^{(\alpha)}(z)\sin\left(m\varphi+\varphi_i^{(\alpha)}\right) \\ & -\sum_{i=0}^{\infty}\frac{m}{rt_i^{(\alpha)}}\frac{\varepsilon_z^{(\alpha)}}{\varepsilon_t^{(\alpha)}}\left[a_i^{(\alpha)}J_m\left(\sqrt{t_i^{(\alpha)}}r\right)+b_i^{(\alpha)}N_m\left(\sqrt{t_i^{(\alpha)}}r\right)\right]\cdot\Psi_i^{'(\alpha)}(z)\sin\left(m\varphi+\psi_i^{(\alpha)}\right)\end{aligned} \tag{30}$$

$$\begin{aligned}H_\varphi^{(\alpha)}(r,\varphi,z) = & \sum_{i=1}^{\infty}\frac{m}{r\lambda_i^{(\alpha)}}\left[c_i^{(\alpha)}J_m\left(\sqrt{\lambda_i^{(\alpha)}}r\right) + d_i^{(\alpha)}N_m\left(\sqrt{\lambda_i^{(\alpha)}}r\right)\right]\Phi_i^{'(\alpha)}(z)\cos\left(m\varphi+\varphi_i^{(\alpha)}\right) \\ & -\sum_{i=0}^{\infty}\frac{j\omega\varepsilon_o\varepsilon_z^{(\alpha)}}{\sqrt{t_i^{(\alpha)}}}\left[a_i^{(\alpha)}J'_m\left(\sqrt{t_i^{(\alpha)}}r\right) + b_i^{(\alpha)}N'_m\left(\sqrt{t_i^{(\alpha)}}r\right)\right]\Psi_i^{(\alpha)}(z)\cos\left(m\varphi+\psi_i^{(\alpha)}\right)\end{aligned} \tag{31}$$

$$E_r^{(\alpha)}(r,\varphi,z) = \sum_{i=0}^{\infty} \frac{1}{\sqrt{t_i^{(\alpha)}}} \frac{\varepsilon_z^{(\alpha)}}{\varepsilon_t^{(\alpha)}} \left[a_i^{(\alpha)} J'_m\left(\sqrt{t_i^{(\alpha)}} r\right) + b_i^{(\alpha)} N'_m\left(\sqrt{t_i^{(\alpha)}} r\right) \right] \Psi_i^{'(\alpha)}(z) \cos\left(m\varphi + \psi_i^{(\alpha)}\right)$$
$$- \sum_{i=1}^{\infty} \frac{j\omega\mu_o m}{r\lambda_i^{(\alpha)}} \left[c_i^{(\alpha)} J_m\left(\sqrt{\lambda_i^{(\alpha)}} r\right) + d_i^{(\alpha)} N_m\left(\sqrt{\lambda_i^{(\alpha)}} r\right) \right] \Phi_i^{(\alpha)}(z) \cos\left(m\varphi + \varphi_i^{(\alpha)}\right) \quad (32)$$

$$H_r^{(\alpha)}(r,\varphi,z) = \sum_{i=1}^{\infty} \frac{1}{\sqrt{\lambda_i^{(\alpha)}}} \left[c_i^{(\alpha)} J'_m\left(\sqrt{\lambda_i^{(\alpha)}} r\right) + d_i^{(\alpha)} N'_m\left(\sqrt{\lambda_i^{(\alpha)}} r\right) \right] \Phi_i^{'(\alpha)}(z) \sin\left(m\varphi + \varphi_i^{(\alpha)}\right)$$
$$- \sum_{i=0}^{\infty} \frac{j\omega\varepsilon_o\varepsilon_z^{(\alpha)} m}{r t_i^{(\alpha)}} \left[a_i^{(\alpha)} J_m\left(\sqrt{t_i^{(\alpha)}} r\right) + b_i^{(\alpha)} N_m\left(\sqrt{t_i^{(\alpha)}} r\right) \right] \Psi_i^{(\alpha)}(z) \sin\left(m\varphi + \psi_i^{(\alpha)}\right) \quad (33)$$

where: $(\alpha) = I, II, ..., XX$ — an index of the region,

$a_i^{(\alpha)}, b_i^{(\alpha)}, c_i^{(\alpha)}, d_i^{(\alpha)}$ — are complex constants, the amplitudes of different types of field

$\psi_i^{(\alpha)}, \varphi_i^{(\alpha)}$ — constants, and $J'_m(x) = \frac{dJ_m(x)}{dx}$ and $N'_m(x) = \frac{dN_m(x)}{dx}$.

Due to the negligible value of higher terms of the series, the summation can be limited to a finite number of terms N. In the first region, the coefficients of the functions N_m must be equal to zero since $\lim_{x\to 0} |N_m(x)| = \infty$.

$4N$ unknown coefficients $c_i^I, c_i^{II}, d_i^{II}, c_i^{III}$ $(i = 1, 2, ..., N)$ and $4(N+1)$ coefficients $a_i^I, a_i^{II}, b_i^{II}, a_i^{III}$ $(i = 0, 1, 2, ...N)$ have to be determined. They are determined through ensuring the continuity of the tangential components of the field on the borders of regions. For the three regions, the following conditions are obtained:

$$E_z^I(R_1,\varphi,z) - E_z^{II}(R_1,\varphi,z) = 0 \quad (34)$$
$$H_z^I(R_1,\varphi,z) - H_z^{II}(R_1,\varphi,z) = 0 \quad (35)$$
$$E_\varphi^I(R_1,\varphi,z) - E_\varphi^{II}(R_1,\varphi,z) = 0 \quad (36)$$
$$H_\varphi^I(R_1,\varphi,z) - H_\varphi^{II}(R_1,\varphi,z) = 0 \quad (37)$$
$$E_z^{II}(R_2,\varphi,z) - E_z^{III}(R_2,\varphi,z) = 0 \quad (38)$$
$$H_z^{II}(R_2,\varphi,z) - H_z^{III}(R_2,\varphi,z) = 0 \quad (39)$$
$$E_\varphi^{II}(R_2,\varphi,z) - E_\varphi^{III}(R_2,\varphi,z) = 0 \quad (40)$$
$$H_\varphi^{II}(R_2,\varphi,z) - H_\varphi^{III}(R_2,\varphi,z) = 0 \quad (41)$$

In the case of a finite number of terms fulfilling the conditions of equality is impossible for all z and φ. Therefore, these coefficients are determined from the condition that the mean square error (functional) component of the difference on either side of the boundary reached the minimum value. The corresponding functionals have the form (here written for the three regions):

$$F_1 = \int_S \left| E_z^I(R_1,\varphi,z) - E_z^{II}(R_1,\varphi,z) \right|^2 ds \quad (42)$$
$$F_2 = \int_S \left| H_z^I(R_1,\varphi,z) - H_z^{II}(R_1,\varphi,z) \right|^2 ds \quad (43)$$
$$F_3 = \int_S \left| E_\varphi^I(R_1,\varphi,z) - E_\varphi^{II}(R_1,\varphi,z) \right|^2 ds \quad (44)$$
$$F_4 = \int_S \left| H_\varphi^I(R_1,\varphi,z) - H_\varphi^{II}(R_1,\varphi,z) \right|^2 ds \quad (45)$$

$$F_5 = \int_S \left|E_z^{II}(R_2,\varphi,z) - E_z^{III}(R_2,\varphi,z)\right|^2 ds \tag{46}$$

$$F_6 = \int_S \left|H_z^{II}(R_2,\varphi,z) - H_z^{III}(R_2,\varphi,z)\right|^2 ds \tag{47}$$

$$F_7 = \int_S \left|E_\varphi^{II}(R_2,\varphi,z) - E_\varphi^{III}(R_2,\varphi,z)\right|^2 ds \tag{48}$$

$$F_8 = \int_S \left|H_\varphi^{II}(R_2,\varphi,z) - H_\varphi^{III}(R_2,\varphi,z)\right|^2 ds \tag{49}$$

Functionals achieve these minimum values if and only if their derivatives with respect to unknown coefficients are equal to zero (Rayleigh-Ritz method).

For example, functional F_1 can be written as:

$$F_1 = \int_S \left|E_z^I(R_1,\varphi,z) - E_z^{II}(R_1,\varphi,z)\right|^2 ds = \int_0^{2\pi}\int_0^{L'} \left|E_z^I(R_1,\varphi,z) - E_z^{II}(R_1,\varphi,z)\right|^2 dz d\varphi \tag{50}$$

wherein the integral should be extended to the entire cylindrical surface on which the matched fields are from different regions. Assuming designation:

$$g(\varphi,z) = E_z^I(R_1,\varphi,z) - E_z^{II}(R_1,\varphi,z) \text{ one can write :}$$

$$g(\varphi,z) = \sum_{i=1}^{\infty} a_i^I J_m\left(\sqrt{t_i^I}R_1\right)\Psi_i^I(z)\cos\left(m\varphi+\psi_i^I\right) - \sum_{i=1}^{\infty}\left[a_i^{II}J_m\left(\sqrt{t_i^{II}}R_1\right) + b_i^{II}N_m\left(\sqrt{t_i^{II}}R_1\right)\right]\Psi_i^{II}(z)\cos\left(m\varphi+\psi_i^{II}\right)$$

Substituting

$$a_i' = a_i^I J_m\left(\sqrt{t_i^I}R_1\right) \text{ and } b_i' = a_i^{II}J_m\left(\sqrt{t_i^{II}}r\right) + b_i^{II}N_m\left(\sqrt{t_i^{II}}r\right)$$

$$g(\varphi,z) = \sum_{i=1}^{\infty} a_i'\Psi_i^I(z)\cos\left(m\varphi+\psi_i^I\right) - \sum_{i=1}^{\infty} b_i'\Psi_i^{II}(z)\cos\left(m\varphi+\psi_i^{II}\right) \text{ and}$$

$$g(\varphi,z) = \sum_{i=0}^{\infty} a_i'\Psi_i^I(z)\cos\left(m\varphi+\psi_i^I\right) - \sum_{i=0}^{\infty}\Psi_i^{II}(z)\left[\cos(m\varphi)b_i'\cos(\psi_i^{II}) - \sin(m\varphi)b_i'\sin(\psi_i^{II})\right]$$

Substituting $c_i' = b_i'\cos(\psi_i^I)$, $d_i' = b_i'\sin(\psi_i^I)$

$$g(\varphi,z) = \sum_{i=0}^{\infty} a_i'\Psi_i^I(z)\cos\left(m\varphi+\psi_i^I\right) - \sum_{i=0}^{\infty}\Psi_i^{II}(z)\left[c_i''\cos(m\varphi) - d_i'\sin(m\varphi))\right]$$

After differentiation with respect to c_i':

$$\frac{\partial F_1}{\partial c_i^I} = \frac{\partial}{\partial c_i^I}\int_S |g(\varphi,z)|^2\, ds = 2\int_S g(\varphi,z)\frac{\partial g(\varphi,z)}{\partial c_i^I}\, ds$$

$$\frac{\partial F_1}{\partial c_i'} = 2\int_S g(\varphi,z)\Psi_i^{II}(z)\cos(m\varphi)\, ds = 0$$

and with respect to d_i':

$$\frac{\partial F_1}{\partial d_i^I} = \frac{\partial}{\partial d_i^I} \int\limits_S |g(\varphi, z)|^2 \, ds = 2 \int\limits_S g(\varphi, z) \frac{\partial g(\varphi, z)}{\partial d_i^I} \, ds$$

$$\frac{\partial F_1}{\partial d_i^{'}} = 2 \int\limits_S g(\varphi, z) \Psi_i^{II}(z) \sin(m\varphi) \, ds = 0$$

In a similar way, one can proceed with other functionals.

After calculating the integrals with respect to variable z in the range of $\langle 0, L' \rangle$, one obtains $K = 8N + 4$ expressions:

$$2\cos(m\varphi) \left[\sum_{i=1}^{K} w_{ni} x_i \cos \eta_i \right] + 2\sin(m\varphi) \left[\sum_{i=1}^{K} w_{ni} x_i \sin \eta_i \right] \tag{51}$$

$$2\cos(m\varphi) \left[\sum_{i=1}^{K} w_{ni} x_i \sin \eta_i \right] + 2\sin(m\varphi) \left[\sum_{i=1}^{K} w_{ni} x_i \cos \eta_i \right] \tag{52}$$

where: $n = 1, 2, ..., K$, $K = 8N + 4$ and $[x_i] = [a_i^I, c_i^I, a_i^{II}, b_i^{II}, c_i^{II}, d_i^{II}, a_i^{III}, c_i^{III}]$, $[\eta_i] = [\psi_i^I, \varphi_i^I, \psi_i^{II}, \varphi_i^{II}, \psi_i^{II}, \varphi_i^{II}, \psi_i^{III}, \varphi_i^{III}]$.

Equations (51) and (52) after being multiplied by $\cos(m\varphi)$ or $\sin(m\varphi)$ are integrated with respect to the variable φ in the range of $\langle 0, 2\pi \rangle$ and equated to zero. Leaving aside the irrelevant factor of 2π for $m \neq 0$ and 4π for $m = 0$, the resulting equation can be represented in the following form:

$$\tilde{W} \begin{bmatrix} x_1 \cos \eta_1 \\ x_2 \cos \eta_2 \\ ... \\ x_K \cos \eta_K \end{bmatrix} = 0 \tag{53}$$

$$\tilde{W} \begin{bmatrix} x_1 \sin \eta_1 \\ x_2 \sin \eta_2 \\ ... \\ x_K \sin \eta_K \end{bmatrix} = 0 \tag{54}$$

Elements w_{ni} $(n = 1, 2, ..., K)$ constituting the matrix $\tilde{W}$ are given in Table 1 for the three regions and Table 2 for the two regions.

The solutions of these systems of homogeneous equations, having the same coefficients matrix, differ by an unrestricted constant q, i.e.: $q x_i \cos \eta_i = x_i \sin \eta_i$

Since $x_i \neq 0$, then $q = \frac{\sin \eta_i}{\cos \eta_i} = \mathrm{tg}\eta_i$, so all $q = \frac{\sin \eta_i}{\cos \eta_i} = \mathrm{tg}\eta_i$ must be equal in amount, i.e., $\eta_i = \eta_o$ for $i = 1, 2, ..., K$. Finally, the equation, from which one can calculate the unknown coefficients, can be written as follows:

$$\tilde{W} \begin{bmatrix} x_1 \\ x_2 \\ .. \\ x_K \end{bmatrix} = 0 \tag{55}$$

This system has a nonzero solution if and only if its determinant is equal to zero:

$$\det \tilde{W} = 0 \tag{56}$$

The matrix $\tilde{W}$ has, for the three regions, the size of $K = 8N + 4$ and a form of Eq. (57):

$$\tilde{W} = \begin{bmatrix} \tilde{U}^{(1)} & \tilde{U}^{(2)} & \tilde{U}^{(3)} & \tilde{U}^{(4)} \\ \tilde{U}^{(5)} & \tilde{U}^{(6)} & \tilde{U}^{(7)} & \tilde{U}^{(8)} \end{bmatrix} \tag{57}$$

Table 1. Elements of W matrix for three regions.

	$\mathbf{l=1}$	$\mathbf{l=2}$	$\mathbf{l=3}$
$v_{ni}^{(1,l)}$ $n,i=0,1,2,...$	$J_m(\sqrt{t_i^I}R_1)\cdot$ $\langle\Psi_i^I,\Psi_n^{II*}\rangle$	$J_m(\sqrt{t_i^{II}}R_1)\cdot$ $\langle\Psi_i^{II},\Psi_n^{II*}\rangle$	$N_m(\sqrt{t_i^{II}}R_1)\cdot$ $\langle\Psi_i^{II},\Psi_n^{II*}\rangle$
$v_{ni}^{(3,l)}$ $n=1,2,3,...$ $i=0,1,2,...$	$\frac{-m}{R_1t_i^I}J_m(\sqrt{t_i^I}R_1)\cdot$ $\langle\frac{\varepsilon_z^I}{\varepsilon_t^I}\Psi_i'^I,\Phi_n^{II*}\rangle$	$\frac{-m}{R_1t_i^{II}}J_m(\sqrt{t_i^{II}}R_1)\cdot$ $\langle\frac{\varepsilon_z^{II}}{\varepsilon_t^{II}}\Psi_i'^{II},\Phi_n^{II*}\rangle$	$\frac{-m}{R_1t_i^{II}}N_m(\sqrt{t_i^{II}}R_1)\cdot$ $\langle\frac{\varepsilon_z^{II}}{\varepsilon_t^{II}}\Psi_i'^{II},\Phi_n^{II*}\rangle$
$v_{ni}^{(4,l)}$ $n,i=0,1,2,...$	$\frac{\omega\varepsilon_o}{\sqrt{t_i^I}}J_m'(\sqrt{t_i^I}R_1)\cdot$ $\langle\varepsilon_z^I\Psi_i^I,\varepsilon_z^{I*}\Psi_n^{I*}\rangle$	$\frac{\omega\varepsilon_o}{\sqrt{t_i^{II}}}J_m'(\sqrt{t_i^{II}}R_1)\cdot$ $\langle\varepsilon_z^{II}\Psi_i^{II},\varepsilon_z^{I*}\Psi_n^{I*}\rangle$	$\frac{\omega\varepsilon_o}{\sqrt{t_i^{II}}}N_m'(\sqrt{t_i^{II}}R_1)\cdot$ $\langle\varepsilon_z^{II}\Psi_i^{II},\varepsilon_z^{I*}\Psi_n^{I*}\rangle$
$v_{ni}^{(6,l)}$ $n,i=1,2,3,...$	$J_m(\sqrt{\lambda_i^I}R_1)\cdot$ $\langle\Phi_i^I,\Phi_n^{I*}\rangle$	$J_m(\sqrt{\lambda_i^{II}}R_1)\cdot$ $\langle\Phi_i^{II},\Phi_n^{I*}\rangle$	$N_m(\sqrt{\lambda_i^{II}}R_1)\cdot$ $\langle\Phi_i^{II},\Phi_n^{I*}\rangle$
$v_{ni}^{(7,l)}$ $n,i=0,1,2,...$	$\frac{\omega\mu_o}{\sqrt{\lambda_i^I}}J_m'(\sqrt{\lambda_i^I}R_1)\cdot$ $\langle\Phi_i^I,\Phi_n^{II*}\rangle$	$\frac{\omega\mu_o}{\sqrt{\lambda_i^{II}}}J_m'(\sqrt{\lambda_i^{II}}R_1)\cdot$ $\langle\Phi_i^{II},\Phi_n^{II*}\rangle$	$\frac{\omega\mu_o}{\sqrt{\lambda_i^{II}}}N_m'(\sqrt{\lambda_i^{II}}R_1)\cdot$ $\langle\Phi_i^{II},\Phi_n^{II*}\rangle$
$v_{ni}^{(8,l)}$ $n=1,2,3,...$ $i=0,1,2,...$	$\frac{m}{R_1\lambda_i^I}J_m(\sqrt{\lambda_i^I}R_1)\cdot$ $\langle\Phi_i'^I,\varepsilon_z^{I*}\Psi_n^{I*}\rangle$	$\frac{m}{R_1\lambda_i^{II}}J_m(\sqrt{\lambda_i^{II}}R_1)\cdot$ $\langle\Phi_i'^{II},\varepsilon_z^{I*}\Psi_n^{I*}\rangle$	$\frac{m}{R_1\lambda_i^{II}}N_m(\sqrt{\lambda_i^{II}}R_1)\cdot$ $\langle\Phi_i'^{II},\varepsilon_z^{I*}\Psi_n^{I*}\rangle$
	$\mathbf{l=6}$	$\mathbf{l=7}$	$\mathbf{l=8}$
$v_{ni}^{(1,l)}$ $n,i=0,1,2,...$	$J_m(\sqrt{t_i^{II}}R_2)\cdot$ $\langle\Psi_i^{II},\Psi_n^{III*}\rangle$	$N_m(\sqrt{t_i^{II}}R_2)\cdot$ $\langle\Psi_i^{II},\Psi_n^{III*}\rangle$	$P_m(\sqrt{t_i^{III}}R_2)\cdot$ $\langle\Psi_i^{III},\Psi_n^{III*}\rangle$
$v_{ni}^{(3,l)}$ $n=1,2,3,...$ $i=0,1,2,...$	$\frac{-m}{R_2t_i^{II}}N_m(\sqrt{t_i^{II}}R_2)\cdot$ $\langle\frac{\varepsilon_z^{II}}{\varepsilon_t^{II}}\Psi_i'^{II},\Phi_n^{III*}\rangle$	$\frac{-m}{R_2t_i^{II}}J_m(\sqrt{t_i^{II}}R_2)\cdot$ $\langle\frac{\varepsilon_z^{II}}{\varepsilon_t^{II}}\Psi_i'^{II},\Phi_n^{III*}\rangle$	$\frac{-m}{R_2t_i^{III}}P_m(\sqrt{t_i^{III}}R_2)\cdot$ $\langle\frac{\varepsilon_z^{III}}{\varepsilon_t^{III}}\Psi_i'^{III},\Phi_n^{III*}\rangle$
$v_{ni}^{(4,l)}$ $n,i=0,1,2,...$	$\frac{\omega\varepsilon_o}{\sqrt{t_i^{II}}}J_m'(\sqrt{t_i^{II}}R_2)\cdot$ $\langle\varepsilon_z^{II}\Psi_i^{II},\varepsilon_z^{II*}\Psi_n^{II*}\rangle$	$\frac{\omega\varepsilon_o}{\sqrt{t_i^{II}}}N_m'(\sqrt{t_i^{II}}R_2)\cdot$ $\langle\varepsilon_z^{II}\Psi_i^{II},\varepsilon_z^{II*}\Psi_n^{II*}\rangle$	$\frac{\omega\varepsilon_o}{\sqrt{t_i^{III}}}P_m'(\sqrt{t_i^{III}}R_2)\cdot$ $\langle\varepsilon_z^{III}\Psi_i^{III},\varepsilon_z^{II*}\Psi_n^{II*}\rangle$
$v_{ni}^{(6,l)}$ $n,i=1,2,3,...$	$J_m(\sqrt{\lambda_i^{II}}R_2)\cdot$ $\langle\Phi_i^{II},\Phi_n^{II*}\rangle$	$N_m(\sqrt{\lambda_i^{II}}R_2)\cdot$ $\langle\Phi_i^{II},\Phi_n^{II*}\rangle$	$Q_m(\sqrt{\lambda_i^{III}}R_2)\cdot$ $\langle\Phi_i^{III},\Phi_n^{II*}\rangle$
$v_{ni}^{(7,l)}$ $n,i=0,1,2,...$	$\frac{\omega\mu_o}{\sqrt{\lambda_i^{II}}}J_m'(\sqrt{\lambda_i^{II}}R_2)\cdot$ $\langle\Phi_i^{II},\Phi_n^{III*}\rangle$	$\frac{\omega\mu_o}{\sqrt{\lambda_i^{II}}}N_m'(\sqrt{\lambda_i^{II}}R_2)\cdot$ $\langle\Phi_i^{II},\Phi_n^{III*}\rangle$	$\frac{\omega\mu_o}{\sqrt{\lambda_i^{III}}}Q_m'(\sqrt{\lambda_i^{III}}R_2)\cdot$ $\langle\Phi_i^{III},\Phi_n^{III*}\rangle$
$v_{ni}^{(7,l)}$ $n=1,2,3,...$ $i=0,1,2,...$	$\frac{m}{R_2\lambda_i^{II}}J_m(\sqrt{\lambda_i^{II}}R_2)\cdot$ $\langle\Phi_i'^{II},\varepsilon_z^{II*}\Psi_n^{II*}\rangle$	$\frac{m}{R_2\lambda_i^{II}}N_m(\sqrt{\lambda_i^{II}}R_2)\cdot$ $\langle\Phi_i'^{II},\varepsilon_z^{II*}\Psi_n^{II*}\rangle$	$\frac{m}{R_2\lambda_i^{III}}Q_m(\sqrt{\lambda_i^{III}}R_2)\cdot$ $\langle\Phi_i'^{III},\varepsilon_z^{II*}\Psi_n^{II*}\rangle$

where for R_3 finite: $P_m(\sqrt{t_i^{III}}r) = N_m(\sqrt{t_i^{III}}R_3)J_m(\sqrt{t_i^{III}}r) - J_m(\sqrt{t_i^{III}}R_3)N_m(\sqrt{t_i^{III}}r)$ and $Q_m(\sqrt{\lambda_i^{III}}r) = N_m'(\sqrt{\lambda_i^{III}}R_3)J_m(\sqrt{\lambda_i^{III}}r) - J_m'(\sqrt{\lambda_i^{III}}R_3)N_m(\sqrt{\lambda_i^{III}}r)$, and for R_3 infinite: $P_m(\sqrt{t_i^{III}}r) = K_m(\sqrt{t_i^{III}}r)$, and $Q_m(\sqrt{\lambda_i^{III}}r) = K_m(\sqrt{\lambda_i^{III}}r)$.

The matrices $\tilde{U}^{(l)}$ ($l = 1, 2, 3, 4, 5, 6, 7, 8$) have the size of $(4N + 2)(2N + 1)$ each. The matrices $\tilde{U}^{(4)}$ and $\tilde{U}^{(5)}$ are the matrices with zero elements, and the remaining matrices are in the form of:

$$\tilde{U}^{(l)} = \begin{bmatrix} \tilde{v}^{(1,l)} & \tilde{v}^{(5,l)} \\ \tilde{v}^{(2,l)} & \tilde{v}^{(6,l)} \\ \tilde{v}^{(3,l)} & \tilde{v}^{(7,l)} \\ \tilde{v}^{(4,l)} & \tilde{v}^{(8,l)} \end{bmatrix}$$

All elements of matrices $\tilde{v}^{(2,l)}\, i\, \tilde{v}^{(5,l)}$ are equal to zero. The non-zero elements of matrices are shown in Table 1.

In a case of two regions, matrix $\tilde{W}$ has a size of $K = 4N + 2$ and a form:

$$\tilde{W} = \begin{bmatrix} \tilde{U}^{(1)} & \tilde{U}^{(2)} \end{bmatrix}$$

The matrices $\tilde{U}^{(l)}$ ($l = 1, 2$) have the same form as above, and the elements of the matrix $\tilde{v}^{(2,l)}$ are presented in Table 2.

Table 2. Elements of W matrix for two regions.

$n \backslash i$	$l = 1$	$l = 2$
$v_{ni}^{(1,l)}$ $n, i = 0, 1, 2, ...$	$J_m(\sqrt{t_i^I} R_1) \cdot \langle \Psi_i^I, \Psi_n^{II*} \rangle$	$P_m(\sqrt{t_i^{II}} R_1) \cdot \langle \Psi_i^{II}, \Psi_n^{II*} \rangle$
$v_{ni}^{(3,l)}$ $n = 1, 2, 3, ...,$ $i = 0, 1, 2, ...$	$\frac{-m}{R_1 t_i^I} J_m(\sqrt{t_i^I} R_1) \cdot \langle \frac{\varepsilon_z^I}{\varepsilon_t^I} \Psi_i'^I, \Phi_n^{II*} \rangle$	$\frac{-m}{R_1 t_i^{II}} P_m(\sqrt{t_i^{II}} R_1) \cdot \langle \frac{\varepsilon_z^{II}}{\varepsilon_t^{II}} \Psi_i'^{II}, \Phi_n^{II*} \rangle$
$v_{ni}^{(4,l)}$ $n, i = 0, 1, 2, ...$	$\frac{\omega \varepsilon_o}{\sqrt{t_i^I}} J_m'(\sqrt{t_i^I} R_1) \cdot \langle \varepsilon_z^I \Psi_i^I, \varepsilon_z^{I*} \Psi_n^{I*} \rangle$	$\frac{\omega \varepsilon_o}{\sqrt{t_i^{II}}} P_m'(\sqrt{t_i^{II}} R_1) \cdot \langle \varepsilon_z^{II} \Psi_i^{II}, \varepsilon_z^{I*} \Psi_n^{I*} \rangle$
$v_{ni}^{(6,l)}$ $n, i = 1, 2, 3, ...$	$J_m(\sqrt{\lambda_i^I} R_1) \cdot \langle \Phi_i^I, \Phi_n^{I*} \rangle$	$Q_m(\sqrt{\lambda_i^{II}} R_1) \cdot \langle \Phi_i^{II}, \Phi_n^{I*} \rangle$
$v_{ni}^{(7,l)}$ $n, i = 0, 1, 2, ...$	$\frac{\omega \mu_o}{\sqrt{\lambda_i^I}} J_m'(\sqrt{\lambda_i^I} R_1) \cdot \langle \Phi_i^I, \Phi_n^{II*} \rangle$	$\frac{\omega \mu_o}{\sqrt{\lambda_i^{II}}} Q_m'(\sqrt{\lambda_i^{II}} R_1) \cdot \langle \Phi_i^{II}, \Phi_n^{II*} \rangle$
$v_{ni}^{(8,l)}$ $n = 1, 2, 3, ...,$ $i = 0, 1, 2, ...$	$\frac{m}{R_1 \lambda_i^I} J_m(\sqrt{\lambda_i^I} R_1) \cdot \langle \Phi_i'^I, \varepsilon_z^{I*} \Psi_n^{I*} \rangle$	$\frac{m}{R_1 \lambda_i^{II}} Q_m(\sqrt{\lambda_i^{II}} R_1) \cdot \langle \Phi_i'^{II}, \varepsilon_z^{I*} \Psi_n^{I*} \rangle$

where: for R_3 finite: $P_m(\sqrt{t_i^{II}} r) = N_m(\sqrt{t_i^{II}} R_2) J_m(\sqrt{t_i^{II}} r) - J_m(\sqrt{t_i^{II}} R_2) N_m(\sqrt{t_i^{II}} r)$ and $Q_m(\sqrt{\lambda_i^{II}} r) = N_m'(\sqrt{\lambda_i^{II}} R_2) J_m(\sqrt{\lambda_i^{II}} r) - J_m'(\sqrt{\lambda_i^{II}} R_2) N_m(\sqrt{\lambda_i^{II}} r)$, and for R_3 infinite: $P_m(\sqrt{t_i^{II}} r) = K_m(\sqrt{t_i^{II}} r)$, and $Q_m(\sqrt{\lambda_i^{II}} r) = K_m(\sqrt{\lambda_i^{II}} r)$.

From Eq. (56) one can determine the complex resonant pulsation with any accuracy and calculate unknown coefficients corresponding to the distribution of the electromagnetic field. For $N = \infty$, the solution is exact, and for N finite accuracy of the solution and the convergence of the method is dependent on N and increases with N. In practice, it is enough to use $N = 5 \div 10$.

On the basis of this solution, a computer program has been developed and implemented that allows the calculation of the resonator made up of 20 regions with 20 layers each. In this case, the matrix has a size of $K = 76N + 38$. In general, for M regions $K = (M - 1)(4N + 2)$.

3. EXAMPLES OF OBTAINED RESULTS

Based on the above theoretical solution, a computer program has been developed and implemented to calculate a resonance frequency of all modes in the resonator containing multilayered media with uniaxial anisotropy. The correctness of the developed program was checked by making a series of calculations and comparing with results obtained by other methods, from other authors and measurements.

Table 3 shows a comparison of the results obtained by means of the program developed by the author and the published data [10, 12].

Table 3. Comparison of resonant frequencies of structures obtained by means of different methods and measurements.

Sample	Mode	$TM_{01\delta}$	$EH_{11\delta}$	$HE_{11\delta}$	$TE_{01\delta}$	HE_{210}
1	f_o [GHz] Publication [12]	7.339	8.827	9.121	9.720	-
	f_o [GHz] Measurement	7.275	8.797	9.009	9.714	-
	f_o [GHz] Described metod	7.339	8.828	9.121	9.719	-
2	f_o [GHz] Publication [12]	10.664	9.841	12.153	10.704	-
	f_o [GHz] Measurement	10.577	9.795	12.138	10.706	-
	f_o [GHz] Described metod	10.666	9.842	12.154	10.704	-
3	f_o [GHz] Publication [10]	8.7185	-	-	8.5405	8.6634
	f_o [GHz] Described metod	8.7322	-	-	8.5421	8.6701
Sample parameters						
Sample no. 1: diameter $D = 9.985\,\text{mm}$, height $L = 9.998\,\text{mm}$, $\varepsilon_t = 9.389$, $\varepsilon_z = 11.478$, centrally placed within a metal cylinder having a diameter $d = 15.5\,\text{mm}$, height $h = 13\,\text{mm}$ with stands of the same diameter as the sample located on both sides of the sample, the height $l_1 = 1.501\,\text{mm}$ and a relative permittivity $\varepsilon_1 = 1.031$. Sample no. 2: diameter $D = 10.002\,\text{mm}$, height $L = 5.002\,\text{mm}$, $\varepsilon_t = 9.399$, $\varepsilon_z = 11.553$, located centrally in the cylinder identical as for sample no. 1 with stands of the same diameter as the sample located on both sides of the sample, the amount $l_1 = 3.999\,\text{mm}$ and a relative permittivity $\varepsilon_1 = 1.031$. Sample no. 3: diameter $D = 37.7\,\text{mm}$, height $L = 9.4\,\text{mm}$, $\varepsilon_t = 4.43$, $\varepsilon_z = 4.59$, centrally placed within a metal cylinder having a diameter $d = 140\,\text{mm}$ and height $h = 9.4\,\text{mm}$.						

As shown in Table 3, the calculation results obtained by means of presented method are identical or nearly identical to the results given in [10, 12], which proves the correctness of the developed method.

Resonant frequencies of Table 3 were calculated for the lowest modes that are used in measurements of the material parameters [16]. However, to validate solutions throughout the frequency range calculations were carried out for the higher modes. The results are shown in Tables 4 and 5 and compared

Table 4. Calculation results of resonant frequencies of the sapphire resonator (MM — radial mode matching method, RR — Rayeigh-Ritz method, Meas. — measurement).

$m = 0$	$\mathbf{WGH_{n,m,0}}$			$\mathbf{WGE_{n,m,0}}$		
n	**MM**	**RR**	**Meas.**	**MM**	**RR**	**Meas**
16	72.33	72.17	72.18	72.99	72.91	73.20
17	74.83	74.70	74.70	76.25	76.17	76.50
18	77.36	77.25	77.23	79.50	79.42	79.85
19	79.92	79.83	79.72	82.73	82.66	82.22
20	82.50	82.43	82.38	85.93	85.91	86.38
21	85.11	85.05	84.89	89.52	89.15	89.70
22	87.74	87.69	87.46	92.55	92.38	92.98
23	90.39	90.35	90.18	95.75	95.61	96.20
24	93.06	93.02	92.78	98.98	98.85	99.45
25	95.74	95.71	95.48			
$m = 1$	$\mathbf{WGH_{n,m,0}}$			$\mathbf{WGE_{n,m,0}}$		
	MM	**RR**	**Meas**	**MM**	**RR**	**Meas**
12	71.04	70.75	70.60	71.87	71.75	72.03
13	73.75	73.49	73.34	75.39	75.27	75.62
14	76.48	76.26	76.10	78.88	78.77	79.32
15	79.23	79.04	78.90	82.35	82.26	82.75
16	82.00	81.84	81.70	85.76	85.72	86.27
17	84.80	84.66	84.50	89.54	89.16	89.70
18	87.61	87.49	87.38	92.79	92.59	93.15
19	90.43	90.34	90.20	96.19	96.02	96.60
20	93.27	93.20	92.98	99.60	99.43	99.96
21	96.12	96.06	95.85			
22	98.99	98.94	98.72			

with those obtained by other methods and the measurements. Measurements and calculations were done for a sample of quartz having a diameter $D = 17.2\,\text{mm}$, height $L = 3.07\,\text{mm}$, $\varepsilon_t = 4.43$, $\varepsilon_z = 4.59$, and for a sample of sapphire having a diameter of $D = 9.96\,\text{mm}$, height $L = 1.068\,\text{mm}$, $\varepsilon_t = 9.37$, $\varepsilon_z = 11.35$. Both samples were placed in the open resonator. As one can see by analyzing these values, there is an agreement between the proposed method, other methods, and measurements.

The described method and written program allow to determine resonant frequencies of variety of complicated structures, for example a sphere. The sphere must be divided into many regions and layers with appropriate height and radius. Such division is shown in Fig. 2 and Table 6. The structure is composed of 19 regions and 3 layers in each region. The calculations of resonant frequencies of a sphere having radius 4.5 mm and scalar relative permittivity equal to 36, placed symmetrically in a metal cylinder having radius 30 mm and height 11 mm are presented in Table 7. The sphere has been approximated by 10 and 19 regions for comparison. The obtained results have been compared with resonant frequencies calculated by means of FDTD method using QuickWave electromagnetic simulator.

As shown in Table 7, the calculated results obtained by means of presented method are close to the results achieved by means of FDTD method, which proves the correctness of the developed method. The relative error decreases with an increase in the number of regions as a result of a better approximation of the sphere.

The comparison of the calculation time carried out with the presented method with the calculation

Table 5. Calculation results of resonant frequencies of the quartz resonator (MM — radial mode matching method, RR — Rayeigh-Ritz method, Meas. — measurement).

$m = 0$	$\mathbf{WGH_{n,m,0}}$			$\mathbf{WGE_{n,m,0}}$		
n	**MM**	**RR**	**Meas**	**MM**	**RR**	**Meas**
21				71.44	71.32	71.80
22	71.73	71.72	71.60	74.21	74.09	74.60
23	74.39	74.38	74.24	76.99	76.86	77.35
24	77.06	77.06	76.90	79.76	79.63	80.20
25	79.72	79.74	79.55	82.53	82.40	82.88
26	82.39	82.42	82.20	85.29	85.17	85.65
27	85.06	85.09	84.85	88.05	87.95	88.45
28	87.73	87.76	87.50	90.82	90.70	91.20
29	90.41	90.44	90.18	93.59	93.46	93.99
30	93.08	93.13	92.80	96.33	96.21	96.72
$m = 1$	$\mathbf{WGH_{n,m,1}}$			$\mathbf{WGE_{n,m,1}}$		
n	**MM**	**RR**	**Meas**	**MM**	**RR**	**Meas**
20	76.61	76.48	76.40	75.99	76.15	76.00
21	80.00	78.88	78.88	78.64	78.80	78.66
22	81.40	81.29	81.31	81.27	81.32	81.35
23	83.80	83.71	83.74	83.91	84.06	83.92
24	86.22	86.14	86.18	86.54	86.70	86.60
25	88.65	88.58	88.60	89.18	89.33	89.24
26	91.09	91.03	90.95	91.81	91.96	91.81
27	93.53	93.53	93.45	94.45	94.62	94.45
27	96.00	96.00	95.80			
29	98.47	98.47	98.30			
30	100.95	100.89	100.73			

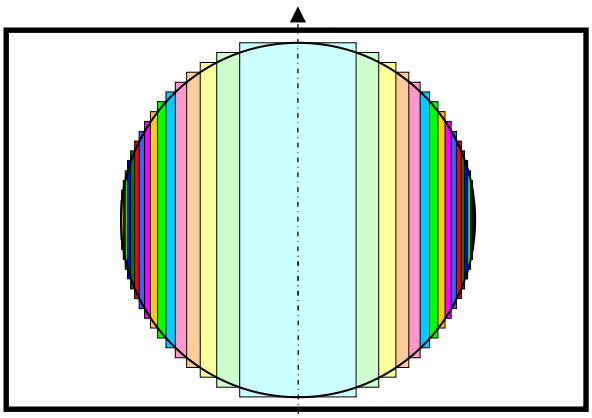

Figure 2. The sphere divided in a radial mode matching method into 18 regions.

time using the QuickWave and CST electromagnetic simulators is presented in Table 8. The calculations were performed for a cylinder and a sphere placed on a dielectric substrate with a relative permeability equal to 2.2. The height of the cylinder was equal to its diameter and was 9 mm. The sphere diameter was also 9 mm. As you can see, the calculation time with the proposed method is several dozen to several hundred times smaller than the calculation time with the simulators used.

Table 6. An approximation of a sphere in presented method.

Region		Layer 1		Layer 2		Layer 3	
No	**Radius [mm]**	**Height [mm]**	**Eps**	**Height [mm]**	**Eps**	**Height [mm]**	**Eps**
1	1.479019946	1	1	9	36	1	1
2	2.061552813	1.25	1	8.5	36	1.25	1
3	2.487468593	1.5	1	8	36	1.5	1
4	2.828427125	1.75	1	7.5	36	1.75	1
5	3.112475	2	1	7	36	2	1
6	3.354102	2.25	1	6.5	36	2.25	1
7	3.561952	2.5	1	6	36	2.5	1
8	3.741657	2.75	1	5.5	36	2.75	1
9	3.897114	3	1	5	36	3	1
10	4.031129	3.25	1	4.5	36	3.25	1
11	4.145781	3.5	1	4	36	3.5	1
12	4.242641	3.75	1	3.5	36	3.75	1
13	4.322904	4	1	3	36	4	1
14	4.387482	4.25	1	2.5	36	4.25	1
15	4.43706	4.5	1	2	36	4.5	1
16	4.472136	4.75	1	1.5	36	4.75	1
17	4.49305	5	1	1	36	5	1
18	4.5	1	1	9	36	1	1
19	30	1	1	9	1	1	1

Table 7. Calculated results of resonant frequencies of dielectric "sphere" placed in metal cylinder.

Regions	Mode	Presented method	FDTD method	Relative error
10	TE_{011}	5.63079347 GHz	5.662 GHz	−0.55116%
10	TM_{011}	6.83878277 GHz	6.734 GHz	1.55603%
19	TE_{011}	5.67101720 GHz	5.701 GHz	−0.52592%
19	TM_{011}	6.89746588 GHz	6.833 GHz	0.94345%

Table 8. The time of calculation of the resonant frequency for a cylinder and a sphere by means of different programs.

Sample	Presented method	FDTD method	CST
Cylinder	0.34 s	12 min	60 s
Sphere	34 s	25 min	8 min

4. CONCLUSIONS

The paper presents in detail the solution of Maxwell's equations for a multilayered dielectric resonator containing the media with uniaxial anisotropy. The radial mode matching method has been used. The results of calculations using the computer program developed have been presented. The results of the calculations are compared with those obtained by other methods, as well as obtained as a result of measurements. These results are in close agreement, which proves the correctness of the method. The solution is developed, and the software program can be used to measure the dielectric permittivity tensor materials and to design advanced dielectric resonators.

REFERENCES

1. Krupka, J., "Frequency domain complex permittivity measurements at microwave frequencies," *Measurement Science and Technology*, Vol. 17, R55–R70, 2006.
2. Abramowicz, A. and J. Modelski, "Dielectric resonators and their applications," PWN, 1990 [in Polish].
3. Courtney, W., "Analysis and evaluation of a method of measuring the complex permittivity and permeability of microwave insulators," *IEEE Trans. on Microwave Theory and Techniques*, Vol. 18, No. 8, 476–485, 1970.
4. Maj, S. and J. Modelski, "Application of a dielectric resonator on microstrip line for measurement of complex permittivity," *IEEE MTT International Microwave Symposium Digest*, 1984.
5. Maj, S., "The method of determining the natural frequency and its application to the analysis of the multilayer cylindrical dielectric resonator," Ph. D thesis, Warsaw, 1987 [in Polish].
6. Derzakowski, K. and A. Abramowicz, "Dielectric resonator figure of merit," *Bulletin of the Polish Academy of Sciences*, Vol. 44, No. 2, 129–139, 1996.
7. www.3ds.com — CST Studio — Electromagnetic field simulation software.
8. www.qwed.eu — Software for Electromagnetic Design.
9. www.ansys.com — 3D Electromagnetic Field Simulator for RF and Wireless Design.
10. Krupka, J., "Resonant modes in shielded cylindrical ferrite and single-crystal dielectric resonators," *IEEE Trans. on Microwave Theory and Techniques*, Vol. 37, No. 4, 691–696, 1989.
11. Tobar, M. and A. Mann, "Resonant frequencies of higher order modes in cylindrical anisotropic dielectric resonators," *IEEE MTT International Microwave Symposium Digest*, 1991.
12. Kobayashi, Y. and T. Sensu, "Resonant modes in shielded uniaxial-anisotropic dielectric rod resonators," *IEEE Trans. on Microwave Theory and Techniques*, Vol. 41, No. 12, 2198–2205, 1993.
13. Krupka, J., et al., "Study of Whispering Gallery modes in anisotropic single-crystal dielectric resonators," *IEEE Trans. on Microwave Theory and Techniques*, Vol. 42, No. 1, 56–61, 1994.
14. Taber, R. and C. Flory, "Microwave oscillators incorporating cryogenic sapphire dielectric resonators," *IEEE Trans. on Ultrasonics, Ferroelectrics, and Frequency Control*, Vol. 42, No. 1, 111–119, 1995.
15. Guan, J. and C. Su, "Resonant frequencies and field distributions for the shielded uniaxially anisotropic dielectric resonator by the FD–SIC method," *IEEE Trans. on Microwave Theory and Techniques*, Vol. 45, No. 10, 1767–1777, 1997.
16. Derzakowski, K., et al., "Whispering gallery resonator method for permittivity measurements," *Journal on Telecommunications and Information Technology*, No. 1, 43–47, 2002.